Supplement of Atmos. Chem. Phys., 21, 17743–17758, 2021
https://doi.org/10.5194/acp-21-17743-2021-supplement

Atmospheric Chemistry and Physics
Open Access
EGU

Supplement of

Responses of surface ozone to future agricultural ammonia emissions and subsequent nitrogen deposition through terrestrial ecosystem changes

Xueying Liu et al.

Correspondence to: Amos P. K. Tai (amostai@cuhk.edu.hk)

S1 Implementation of soil NO_x and NH_3 emission in CLM4.5-BGC

S1.1 Soil NO_x

We incorporate new equations to calculate NO_x released as by-products of nitrification and denitrification. Default CLM estimates the amount of N_2O leakage during nitrification by applying a constant scale factor to the nitrification rate (Li et al., 2000) while that from denitrification is variable and evaluated using the Century approach (Del Grosso et al., 2000). Building on the work of previous studies (Parton et al., 2001, 2004; Zhao et al., 2017), we compute a ratio of NO_x to N_2O to account for the leaking of the former during nitrification and denitrification using the following equations:

$$\mathrm{NO}_x:\mathrm{N_2O} = 15.2 + \frac{35.5\tan^{-1}[0.68\pi(10D_\mathrm{r} - 1.86)]}{\pi} \quad \text{Eq. 1}$$

where D_r is the relative gas diffusivity of soil vs. air and is calculated as a function of air-filled pore space (AFPS) of soil (Davidson and Trumbore, 1995):

$$D_\mathrm{r} = 0.209\mathrm{AFPS}^{\frac{4}{3}} \quad \text{Eq. 2}$$

$$\mathrm{AFPS} = 1 - \frac{\theta_\mathrm{V}}{\theta_\mathrm{V,sat}} \quad \text{Eq. 3}$$

where θ_V and $\theta_\mathrm{V,sat}$ are instantaneous and saturated volumetric soil water content (in m^3 m^{-3}), respectively.

In addition, we also rectify a coding mistake in CLM by restoring a missing 20% of microbial mineralized nitrogen for nitrification to correct the rapid denitrification in previous versions (Parton et al., 2001), and applied a temperature factor to correct the overestimation at high latitudes as suggested in some previous studies (Xu and Prentice, 2008; Zhao et al., 2017):

$$f_T = \min\left(1, e^{308.56\left(\frac{1}{68.02} - \frac{1}{T_\mathrm{soil}+46.02}\right)}\right) \quad \text{Eq. 4}$$

where T_soil is soil temperature in Kelvin (K).

S1.2 Soil NH_3

We add into this model a new NH_3 emission scheme consistent with another standalone biogeochemical model, DNDC version 9.5 (Li et al., 2012), which has been used for studying agricultural NH_3 emission (Balasubramanian et al., 2015, 2017; Zhang and Niu, 2016).

For each model soil layer, NH_3 volatilization is considered as a multistage process, which is formulated as:

$$\frac{\mathrm{d}\left[\mathrm{NH_{3\,(g)}}\right]}{\mathrm{d}t}_\mathrm{soil} = \left[\mathrm{NH^+_{4\,(soil)}}\right](1 - f_\mathrm{ads})f_\mathrm{dis}f_\mathrm{vol}\left(\frac{1}{\Delta t}\right) \quad \text{Eq. 5}$$

where $[NH_4^+{}_{(soil)}]$ (in g-N m^{-2}) is the amount of soil NH_4^+; Δt is model time step size in CLM (default = 30 min or 1800 s).

Due to electrostatic attraction, a portion of soil NH_4^+ adsorbs on the naturally negatively charged surface of soil particles. Our scheme estimates the fraction of NH_4^+ adsorbed, f_ads, as:

$$f_{\mathrm{ads}} = 0.99(7.2733 f_{\mathrm{clay}}^3 - 11.22 f_{\mathrm{clay}}^2 + 5.7198 f_{\mathrm{clay}} + 0.0263) \quad \text{Eq. 6}$$

where f_{clay} is soil clay fraction as prescribed by the CLM surface data (Bonan et al., 2002).

The non-adsorbed NH_4^+ dissociates reversibly into aqueous NH_3 and hydrogen ion ($NH_4^+{}_{(aq)} \rightleftharpoons NH_3{}_{(aq)} + H^+$). The fraction of such NH_4^+ dissociated into aqueous NH_3, f_{dis}, is determined by the following equations (Li et al., 2012):

$$f_{\mathrm{dis}} = \frac{K_{\mathrm{w}}}{K_{\mathrm{a}}[\mathrm{H}^+]} \quad \text{Eq. 7}$$

$$K_{\mathrm{w}} = 10^{0.08946 + 0.03605 T_{\mathrm{soil}}} \times 10^{-15} \quad \text{Eq. 8}$$

$$K_{\mathrm{a}} = (1.416 + 0.01357 T_{\mathrm{soil}}) \times 10^{-5} \quad \text{Eq. 9}$$

$$[\mathrm{H}^+] = 10^{-\mathrm{pH}} \quad \text{Eq. 10}$$

where K_a (in mol L^{-1}) and K_w (in mol L^{-2}) are dissociation constants for NH_4^+/NH_3 and hydrogen-/hydroxide-ion equilibria, respectively; T_{soil} (in ºC) is soil temperature; $[H^+]$ (in mol) is the concentration of aqueous hydrogen ion in the soil calculated from soil pH. The model has yet to be capable of calculating soil pH implicitly, and NH_3 volatilization is sensitive to soil pH, so we perform our simulations using a constant pH of 6.8, as is adopted by DNDC, for a more concise analysis.

Lastly, we use this equation to calculate the fraction of aqueous NH_3 volatilized as gaseous NH_3, f_{vol}:

$$f_{\mathrm{vol}} = \left(\frac{1.5s}{1+s}\right)\left(\frac{T_{\mathrm{soil}}}{50 + T_{\mathrm{soil}}}\right)\left(\frac{l_{\mathrm{max}} - l}{l_{\mathrm{max}}}\right) \quad \text{Eq. 11}$$

where s (in m s^{-1}) is surface wind speed; T_{soil} (in ºC) is soil temperature; l and l_{max} (both in m) are the depth of each particular soil layer and the maximum depth of a soil column, respectively.

S2 Supplementary figures

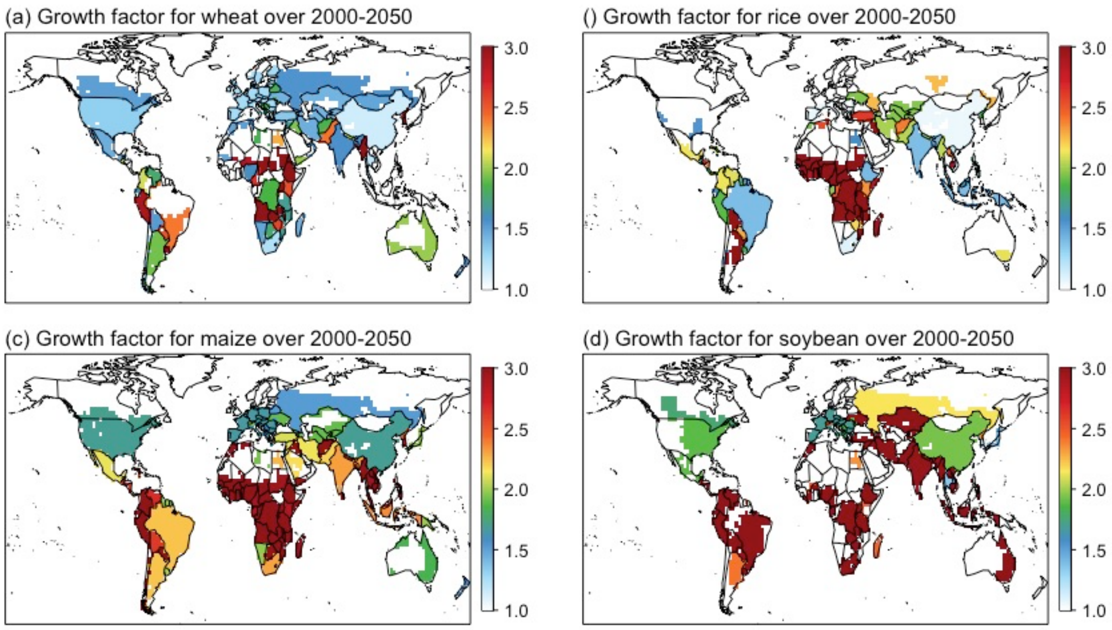

Figure S1. Growth factor of (a) wheat, (b) rice, (c) maize, and (d) soybean production increases over 2000–2050 from the Food and Agriculture Organization of the United Nations (FAO).

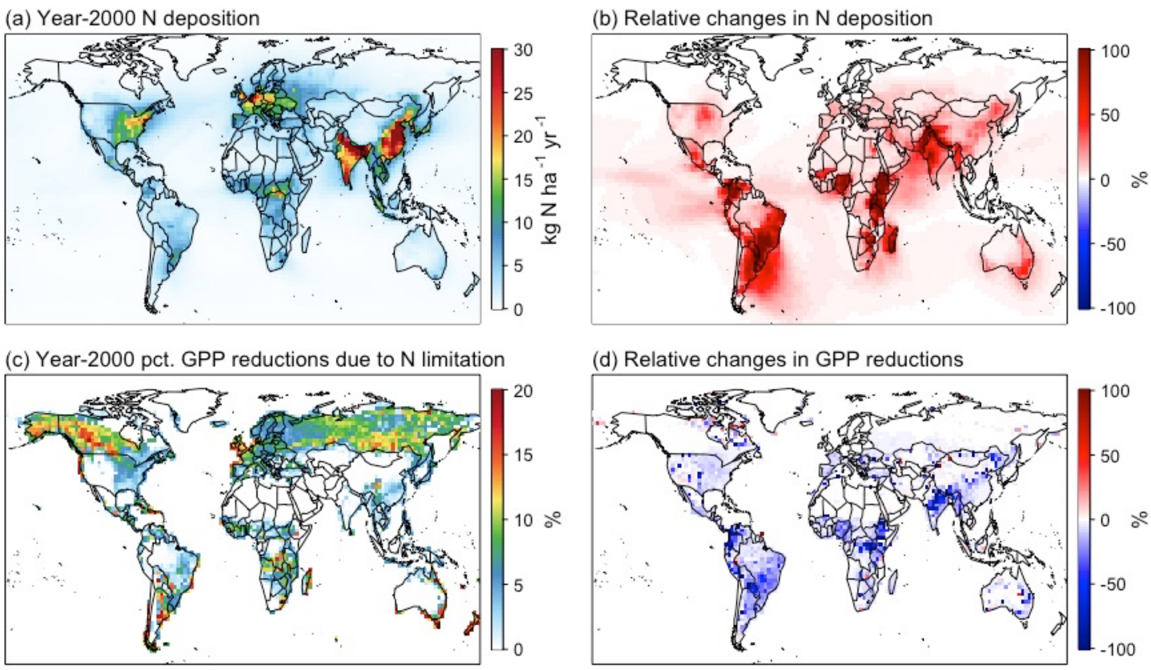

Figure S2. (a) Year-2000 atmospheric nitrogen deposition and **(b)** relative changes in nitrogen deposition over 2000–2050. **(c)** Year-2000 gross primary production (GPP) percentage reduction due to nitrogen limitation as presented in the CLM model. In nitrogen-limited soils (i.e., colored areas), plant growth is limited by insufficient soil nitrogen supply due to plant-microbe competition. **(d)** Relative changes in nitrogen limitation-induced GPP reductions because of enhanced nitrogen availability from atmospheric nitrogen deposition over 2000–2050. Same as Fig.3 but in relative changes.

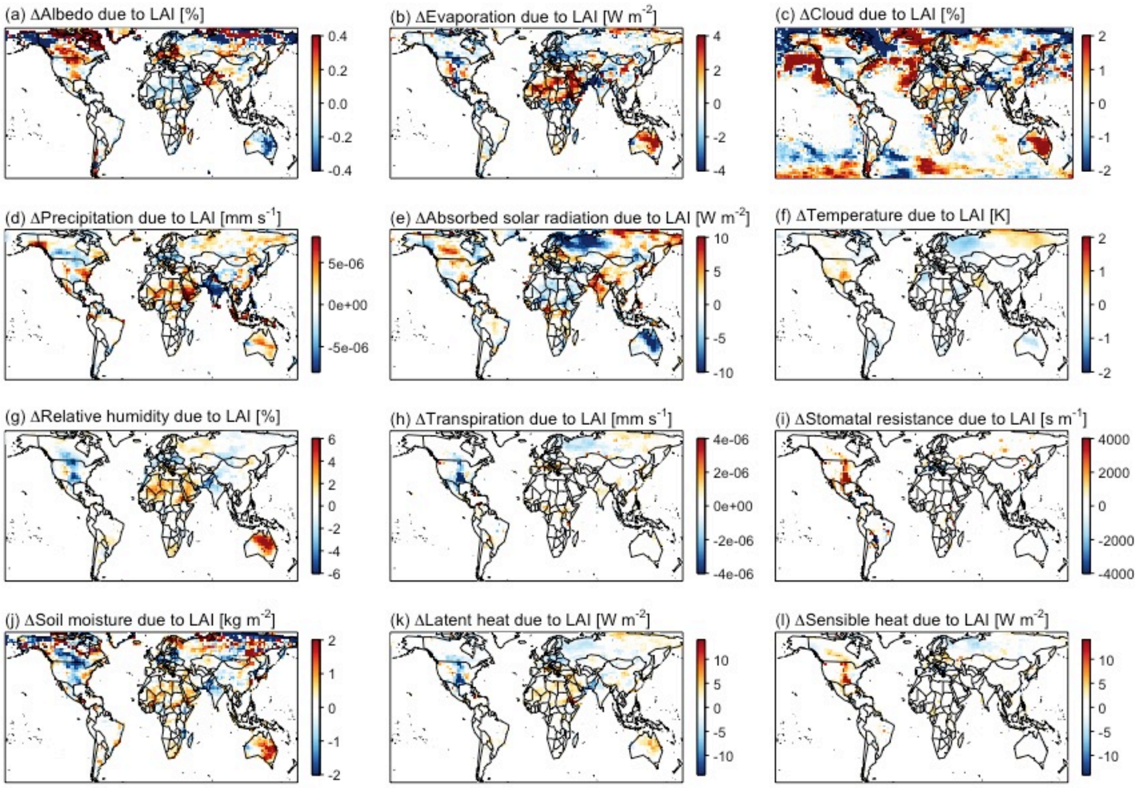

Figure S3. Summertime changes in **(a)** albedo, **(b)** ground evaporation, **(c)** cloud cover, **(d)** precipitation, **(e)** absorbed solar radiation, **(f)** surface temperature, **(g)** relative humidity, **(h)** vegetation transpiration, **(i)** stomatal resistance, **(j)** soil moisture, **(k)** latent heat flux, and **(l)** sensible heat flux driven by LAI increase with dynamic meteorology.

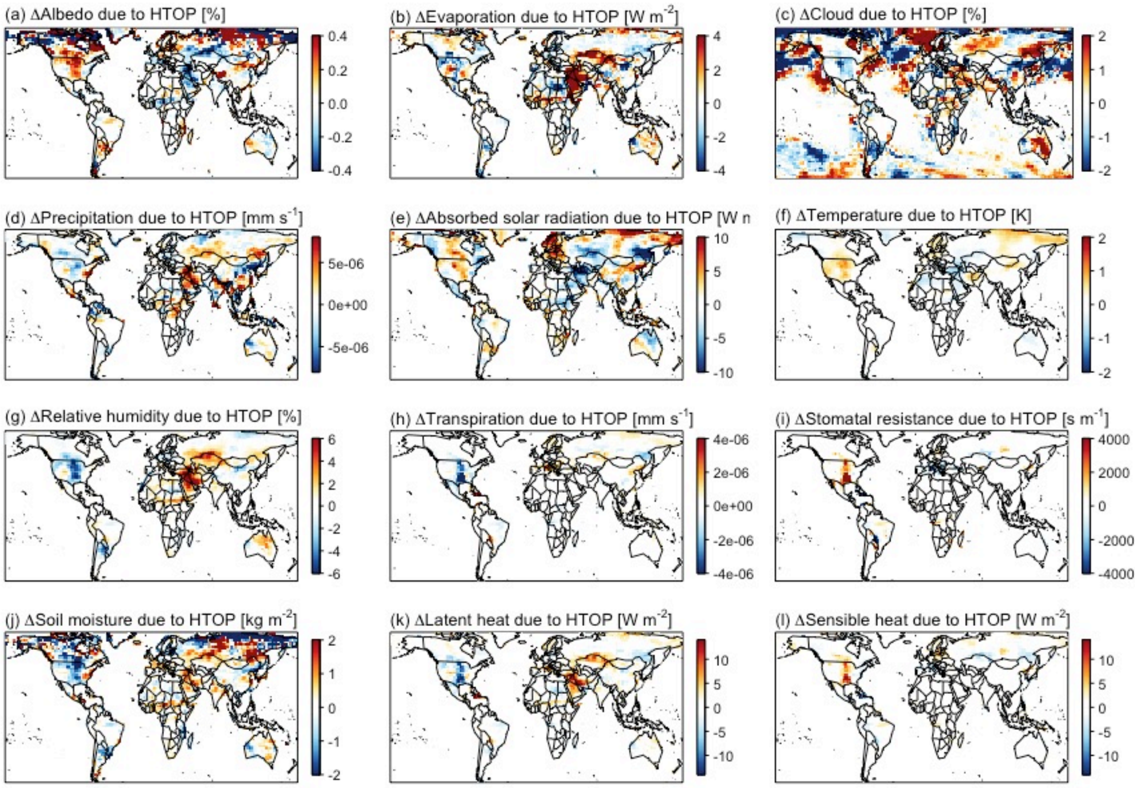

Figure S4. Same as Fig.S3 but driven by canopy height increase.

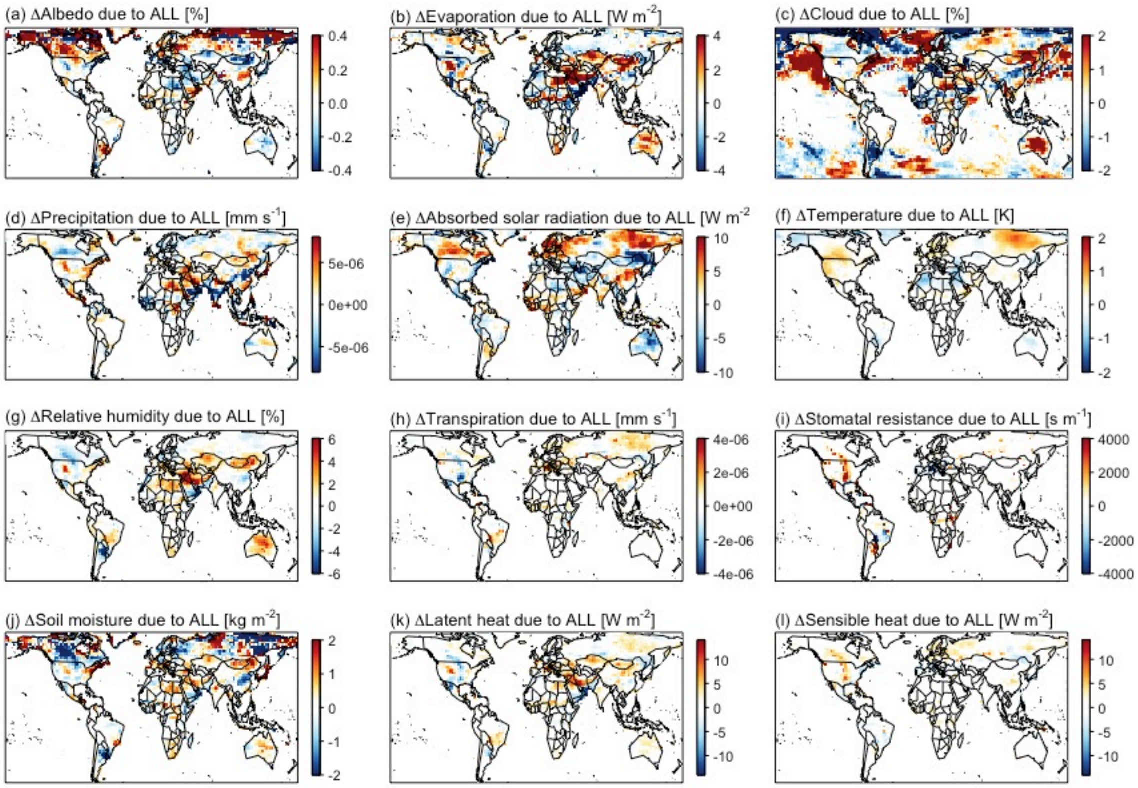

Figure S5. Same as Fig.S3 but driven by LAI, canopy height, and soil NO_x increase.

Reference:

Balasubramanian, S., Koloutsou-Vakakis, S., McFarland, D. M. and Rood, M. J.: Reconsidering emissions of ammonia from chemical fertilizer usage in midwest USA, J. Geophys. Res., 120(12), 6232–6246, doi:10.1002/2015JD023219, 2015.

Balasubramanian, S., Nelson, A., Koloutsou-Vakakis, S., Lin, J., Rood, M. J., Myles, L. T. and Bernacchi, C.: Evaluation of DeNitrification DeComposition model for estimating ammonia fluxes from chemical fertilizer application, Agric. For. Meteorol., 237–238, 123–134, doi:10.1016/j.agrformet.2017.02.006, 2017.

Bonan, G. B., Levis, S., Kergoat, L. and Oleson, K. W.: Landscapes as patches of plant functional types: An integrating concept for climate and ecosystem models, Global Biogeochem. Cycles, 16(2), 5-1-5–23, doi:10.1029/2000gb001360, 2002.

Davidson, E. A. and Trumbore, S. E.: Gas diffusivity and production of CO2 in deep soils of the eastern Amazon, Tellus B, 47(5), 550–565, doi:10.1034/j.1600-0889.47.issue5.3.x, 1995.

Del Grosso, S. J., Parton, W. J., Mosier, A. R., Ojima, D. S., Kulmala, A. E. and Phongpan, S.: General model for N2O and N2 gas emissions from soils due to dentrification, Global Biogeochem. Cycles, 14(4), 1045–1060, doi:10.1029/1999GB001225, 2000.

Li, C., Aber, J., Stange, F., Butterbach-Bahl, K. and Papen, H.: A process-oriented model of N 2 O and NO emissions from forest soils: 1. Model development, J. Geophys. Res. Atmos., 105(D4), 4369–4384, doi:10.1029/1999JD900949, 2000.

Li, C., Salas, W., Zhang, R., Krauter, C., Rotz, A. and Mitloehner, F.: Manure-DNDC: A biogeochemical process model for quantifying greenhouse gas and ammonia emissions from livestock manure systems, Nutr. Cycl. Agroecosystems, 93(2), 163–200, doi:10.1007/s10705-012-9507-z, 2012.

Parton, W. J., Holland, E. A., Del Grosso, S. J., Hartman, M. D., Martin, R. E., Mosier, A. R., Ojima, D. S. and Schimel, D. S.: Generalized model for NO_x and N_2O emissions from soils, J. Geophys. Res. Atmos., 106(D15), 17403–17419, doi:10.1029/2001JD900101, 2001.

Parton, W. J., Holland, E. A., Del Grosso, S. J., Hartman, M. D., Martin, R. E., Mosier, A. R., Ojima, D. S. and Schimel, D. S.: Generalized model for NOx and N2O emissions from soils , J. Geophys. Res. Atmos., 106(D15), 17403–17419, doi:10.1029/2001jd900101, 2004.

Xu, R. and Prentice, I. C.: Terrestrial nitrogen cycle simulation with a dynamic global vegetation model, Glob. Chang. Biol., 14(8), 1745–1764, doi:10.1111/j.1365-2486.2008.01625.x, 2008.

Zhang, Y. and Niu, H.: The development of the DNDC plant growth sub-model and the application of DNDC in agriculture: A review, Agric. Ecosyst. Environ., 230, 271–282, doi:10.1016/j.agee.2016.06.017, 2016.

Zhao, Y., Zhang, L., Tai, A. P. K., Chen, Y. and Pan, Y.: Responses of surface ozone air quality to anthropogenic nitrogen deposition in the Northern Hemisphere, Atmos. Chem. Phys., 17(16), 9781–9796, doi:10.5194/acp-17-9781-2017, 2017.